Fluorescence polarization characterization of biaxial orientation

Philippe Lapersonne, Jean François Tassin*, Philippe Sergot and Lucien Monnerie

Laboratoire de Physicochimie Structurale et Macromoléculaire, Ecole Supérieure de Physique et Chimie Industrielles de Paris, 10 Rue Vauquelin, 75231 Paris Cedex 05, France

and Gilles Le Bourvellec

Rhône-Poulenc Recherches, Centre de Recherches des Carrières, 85 Avenue des Frères Perrets, BP 62, 69192 Saint Fons Cedex, France

(Received 28 September 1988; revised 11 January 1989; accepted 13 January 1989)

A mathematical treatment is proposed to calculate five orientation averages in a biaxially oriented sample from six convenient polarized fluorescence intensities. An experimental method allowing intensity measurements is accurately described and applied to isotropic, uni- and biaxially oriented poly(ethylene terephthalate glycol) films doped with a fluorescent probe.

(Keywords: orientation; fluorescence polarization; poly(ethylene terephthalate glycol))

INTRODUCTION

The development of biaxial orientation in polymers is a common industrial feature in many processing methods, especially in the production of polymer films. Mechanical as well as thermal properties are strongly influenced by the molecular orientation and the morphology of both amorphous and crystalline phases.

Poly(ethylene terephthalate glycol) (PET) films are a stimulating example since they offer a large variety of applications, and undergo stress-induced crystallization under the usual processing conditions. Various reports have already dealt with the characterization of biaxially oriented PET films. Refractive index measurements[1–4] provide a first insight into the overall anisotropy of the material. More specific information concerning each phase is revealed by spectroscopic techniques.

Although orientation averages can be obtained using broad-band n.m.r.[5], high-resolution solid-state n.m.r. techniques have recently been proposed to characterize the orientation in uniaxially[6] and biaxially deformed samples[7]. In the latter case, an accurate description of the average orientation has been achieved, but crystalline and amorphous orientations have not been separated. This separation can be achieved with Raman intensity measurements[2,4,5]. Infra-red spectroscopy, which requires that the sample be tilted[2,5,8,9], can also be used, but only restricted information about the orientation distribution can be obtained. The structure of the crystalline phase can be characterized by X-ray diffraction methods[10–13].

Fluorescence polarization (FP) has previously been used by our group[14,15] and others[16–21] to determine the orientation of fluorescent dyes located in the amorphous phase of uniaxially stretched samples. Some qualitative studies on biaxially oriented films have been reported by Nishijima *et al.*[22,23]. The anisotropy of the intrinsic fluorescence of PET films has also been investigated[24,25]. Nevertheless, the physical origin of this fluorescence is not clearly established and only limited conclusions can be drawn.

The aim of this paper is to present a theoretical and experimental method for characterizing the orientation of a motionless fluorescent probe dispersed in a biaxially oriented material using polarized fluorescence intensity measurements.

THEORETICAL DESCRIPTION OF BIAXIAL ORIENTATION

Hereafter, we will consider the orientation of a fluorescent probe, more precisely the orientation of the transition moment of the probe, with respect to the principal axes of the film. We define a system of axes $0X_1X_2X_3$ attached to the sample. The subscripts 1 and 2 refer to the principal axes in the plane of the film (1 being the machine and 2 the transverse direction), and the $0X_3$ axis is perpendicular to this plane. The orientation of a unit vector $\boldsymbol{M}_0$ (the transition moment direction) can thus be described by the angles θ and φ as illustrated in *Figure 1*. The angle θ gives the preferential orientation along the machine direction while φ yields information about the orientation with respect to the plane of the film. The orientation of the $\boldsymbol{M}_0$ vectors can be defined by an orientation distribution function (ODF) $N(\theta, \varphi)$, where $N(\theta, \varphi) \sin\theta \, d\theta \, d\varphi$ is the fraction of vectors lying in the solid angle $\sin\theta \, d\theta \, d\varphi$. This function can be expanded in a series of spherical harmonic functions as[5,26]:

$$N(\theta, \varphi) = \sum_{l=0}^{\infty} \sum_{m=-l}^{+l} \langle P_{lm0} \rangle Z_{lm0}(\cos\theta) \, e^{-im\varphi} \qquad (1)$$

in which $Z_{lm0}(\cos\theta)$ is a generalized Legendre polynomial and $\langle P_{lm0} \rangle$ is the average of the function

* To whom correspondence should be addressed

0032-3861/89/081558-07$03.00

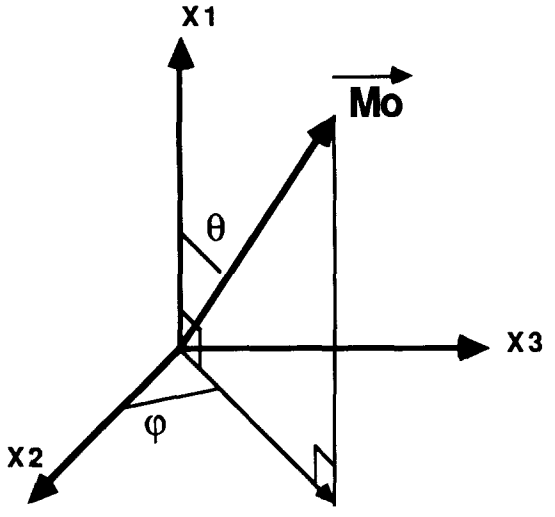

Figure 1 Definition of the θ and φ angles, determining the orientation of the M_0 vector

P_{lm0} (cos θ) taken over the distribution of M_0 units. It will be shown later that the FP technique allows us to measure these coefficients up to the fourth order; for a biaxial symmetry, they are[5]:

$$\langle P_{200}\rangle = \frac{1}{2}\langle 3\cos^2\theta - 1\rangle$$

$$\langle P_{220}\rangle = \frac{1}{4}\langle (1-\cos^2\theta)\cos 2\varphi\rangle$$

$$\langle P_{400}\rangle = \frac{1}{8}\langle 3 - 30\cos^2\theta + 35\cos^4\theta\rangle \qquad (2)$$

$$\langle P_{420}\rangle = \frac{1}{24}\langle (-1+8\cos^2\theta - 7\cos^4\theta)\cos 2\varphi\rangle$$

$$\langle P_{440}\rangle = \frac{1}{16}\langle (1-2\cos^2\theta+\cos^4\theta)\cos 4\varphi\rangle$$

In unambiguous cases, the brackets will be omitted. Using these five averages, an estimate of the ODF can be deduced via the concept of the 'most probable distribution function' introduced by Bower[27,28].

EXPRESSION OF FLUORESCENCE INTENSITIES FOR A BIAXIAL FROZEN SYSTEM

Polarized fluorescence intensities are related to the orientation of the transition moment in both absorption and emission. The fluorescence intensity $I(\boldsymbol{P}, \boldsymbol{A})$ measured when the polarizer and the analyser are set in the directions of the unit vectors $\boldsymbol{P}$ and $\boldsymbol{A}$ respectively is given by[26,29]:

$$I(\boldsymbol{P}, \boldsymbol{A}) = K\langle \cos^2(\boldsymbol{P}.\boldsymbol{M}_a)\cos^2(\boldsymbol{M}_e.\boldsymbol{A})\rangle \qquad (3)$$

where K is an instrumental constant and $\boldsymbol{M}_a$ and $\boldsymbol{M}_e$ are the directions of the transition moment in absorption and emission respectively. Throughout this paper, we assume that the fluorescent probe cannot undergo any motion during the lifetime of the excited state. Furthermore, we first consider the case where $\boldsymbol{M}_a$ and $\boldsymbol{M}_e$ coincide. The effect of the delocalization of the transition moment will be considered later.

The case $\boldsymbol{M}_a = \boldsymbol{M}_e = \boldsymbol{M}_0$

Following the formalism of Desper and Kimura[30], the state of orientation is completely determined by a 3×3 symmetric matrix of reduced intensities I_{ij} defined by:

$$I_{ij} = (1/K)\, I(\boldsymbol{X}_i, \boldsymbol{X}_j) \qquad (4)$$

Owing to the normalization condition:

$$\sum_{i=1}^{3}\sum_{j=1}^{3} I_{ij} = 1 \qquad (5)$$

only five independent reduced intensities are required to characterize a biaxially oriented sample completely. Any other fluorescence intensity for which $\boldsymbol{P}$ and $\boldsymbol{A}$ do not coincide with a principal axis is a linear combination of these reduced intensities. A practical way of measuring these intensities will be described later. Let us now discuss information available from these five intensities.

According to Jarry *et al.*[14], any fluorescence intensity can be expanded as a product of series of spherical harmonics $Y_l^m(\Omega)$:

$$I(\boldsymbol{P}, \boldsymbol{A}) = K\sum_{k=0}^{\infty}\sum_{m=-k}^{+k}\sum_{l=0}^{\infty}\sum_{n=-l}^{+l} p_k^m a_l^n f_{kl}^{mn} \qquad (6)$$

with:

$$f_{kl}^{mn} = \langle \overline{Y_k^m(\Omega)}\, Y_l^n(\Omega)\rangle \qquad (7)$$

and

$$p_k^m = \int \cos^2(\boldsymbol{P}.\boldsymbol{M}_0)\, Y_k^m(\Omega)\, d\Omega$$

$$a_l^n = \int \cos^2(\boldsymbol{A}.\boldsymbol{M}_0)\, \overline{Y_l^n(\Omega)}\, d\Omega \qquad (8)$$

The expansion given in expression (6) can be applied to the I_{ij} intensities referred to above. Owing to symmetry, these intensities are linear combinations of seven mean values:

$$f_{00}^{00} = 1/4\pi \quad f_{20}^{00} \quad f_{20}^{20} = f_{02}^{02} = f_{20}^{-20} = f_0^{0\,-2}_{\;2}$$
$$f_{22}^{20} = f_{22}^{02} = f_{22}^{-20} = f_2^{0\,-2}_{\;2} \quad f_{22}^{00} \quad f_{22}^{22} = f_2^{-2\,-2}_{\;2}$$
$$f_2^{2\,-2}_{\;2} = f^{-22}_{\;22}$$

Since f_{00}^{00} is a constant, it is useful to normalize the f_{kl}^{mn}. We define:

$$G_{20}^{00} = (1/\sqrt{5})(f_{20}^{00}/f_{00}^{00}) = (1/2)\langle 3\cos^2\theta - 1\rangle$$
$$G_{22}^{00} = (1/5)(f_{22}^{00}/f_{00}^{00}) = (1/4)\langle (3\cos^2\theta - 1)^2\rangle$$
$$G_{20}^{20} = (3/\sqrt{30})(f_{20}^{20}/f_{00}^{00}) = (3/4)\langle \sin^2\theta\cos 2\varphi\rangle$$
$$G_{22}^{20} = (3/\sqrt{5}\sqrt{30})(f_{22}^{20}/f_{00}^{00}) = (3/8)\langle (3\cos^2\theta - 1)\sin^2\theta\cos 2\varphi\rangle \qquad (9)$$
$$G_{22}^{22} = (9/30)(f_{22}^{22}/f_{00}^{00}) = (9/16)\langle \sin^4\theta\rangle$$
$$G_2^{2\,-2} = (9/30)(f_2^{2\,-2}/f_{00}^{00}) = (9/16)\langle \sin^4\theta\cos 4\varphi\rangle$$

The reduced fluorescence intensities with respect to the principal axes, I_{ij}, can be written using equations (6–9) as a function of the G_{kl}^{mn}:

$$\begin{pmatrix} 9I_{11}-1 \\ 9I_{22}-1 \\ 9I_{33}-1 \\ 9I_{12}-1 \\ 9I_{13}-1 \\ 9I_{23}-1 \end{pmatrix} = \begin{pmatrix} 4 & 4 & 0 & 0 & 0 & 0 \\ -2 & 1 & 4 & -4 & 2 & 2 \\ -2 & 1 & -4 & 4 & 2 & 2 \\ 1 & -2 & 2 & 4 & 0 & 0 \\ 1 & -2 & -2 & -4 & 0 & 0 \\ -2 & 1 & 0 & 0 & -2 & -2 \end{pmatrix} \begin{pmatrix} G_{20}^{00} \\ G_{22}^{00} \\ G_{20}^{20} \\ G_{22}^{20} \\ G_{22}^{22} \\ G_2^{2\,-2} \end{pmatrix} \qquad (10)$$

We also use the condensed form $I = M \times G$.

Owing to the normalization condition (5), one of these six intensities is redundant. The definition of the G_{kl}^{mn} in (9) shows that one of them can be expressed as a function of the others:

$$G_{22}^{22} = \frac{1}{4} G_{22}^{00} - \frac{1}{2} G_{20}^{00} + \frac{1}{4} \tag{11}$$

so the M matrix can be reduced to a 5×5 matrix M':

$$\begin{pmatrix} 9I_{11}-1 \\ 9I_{22}-3/2 \\ 9I_{33}-3/2 \\ 9I_{13}-1 \\ 9I_{23}-1/2 \end{pmatrix} = \begin{pmatrix} 4 & 4 & 0 & 0 & 0 \\ -3 & 3/2 & 4 & -4 & 2 \\ -3 & 3/2 & -4 & 4 & 2 \\ 1 & -2 & -2 & -4 & 0 \\ -1 & 1/2 & 0 & 0 & -2 \end{pmatrix} \begin{pmatrix} G_{20}^{00} \\ G_{22}^{00} \\ G_{20}^{20} \\ G_{22}^{20} \\ G_2^{2-2} \end{pmatrix}$$

$$I' = M' \times G' \tag{12}$$

The G_{kl}^{mn} and P_{lm0} coefficients are related by the following matrix expression:

$$\begin{pmatrix} P_{200} \\ P_{220} \\ P_{400}+7/18 \\ P_{420} \\ P_{440} \end{pmatrix} = \begin{pmatrix} 1 & 0 & 0 & 0 & 0 \\ 0 & 0 & 1/3 & 0 & 0 \\ -5/9 & 35/18 & 0 & 0 & 0 \\ 0 & 0 & 2/27 & 7/27 & 0 \\ 0 & 0 & 0 & 0 & 1/9 \end{pmatrix} \begin{pmatrix} G_{20}^{00} \\ G_{22}^{00} \\ G_{20}^{20} \\ G_{22}^{20} \\ G_2^{2-2} \end{pmatrix}$$

$$P = M'' \times G' \tag{13}$$

so that:

$$P = M'' \times M'^{-1} \times I' \tag{14}$$

Equation (14) shows that the five moments of the ODF can be determined from a set of five reduced fluorescence intensities.

The case $M_a \neq M_e$

We now analyse the more usual case where an electronic delocalization exists between the absorption and emission moments. We assume that the orientation distribution of vectors M_a is axially symmetric about M_0 and identical to that of M_e about M_0. The validity of this assumption will be discussed later. We also assume that the delocalization is independent of the state of orientation in the sample.

The treatment presented above can still be applied. The coefficients G_{kl}^{mn} of the above treatment become γ_{kl}^{mn} in the presence of delocalization effects. They are related to the true G_{kl}^{mn} by the following relation[14]:

$$\gamma_{20}^{m0} = a G_{20}^{m0} \qquad \gamma_{22}^{mn} = a^2 G_{22}^{mn} \tag{15}$$

where $a = (5r_0/2)^{1/2}$ and r_0 is the fundamental anisotropy of the probe.

The reduced fluorescence intensities I_{ij} can be written in a matrix form similar to equation (10). The normalization condition (5) is still valid and the intensities can be expressed as a function of five G_{kl}^{mn} using a 5×5 matrix:

$$\begin{pmatrix} 9I_{11}-1 \\ 9I_{22}-1-a^2/2 \\ 9I_{33}-1-a^2/2 \\ 9I_{13}-1 \\ 9I_{23}-1+a^2/2 \end{pmatrix} = \begin{pmatrix} 4a & 4a^2 & 0 & 0 & 0 \\ -(2a+a^2) & 3a^2/2 & 4a & -4a^2 & 2a^2 \\ -(2a+a^2) & 3a^2/2 & -4a & 4a^2 & 2a^2 \\ a & -2a^2 & -2a & -4a^2 & 0 \\ -(2a-a^2) & a^2/2 & 0 & 0 & -2a^2 \end{pmatrix} \begin{pmatrix} G_{20}^{00} \\ G_{22}^{00} \\ G_{20}^{20} \\ G_{22}^{20} \\ G_2^{2-2} \end{pmatrix} \tag{16}$$

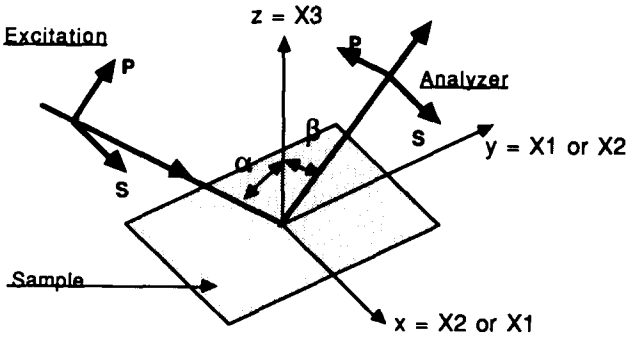

Figure 2 Schematic representation of a suitable device for fluorescence intensity measurements

The five moments P_{lm0} can then be calculated using expression (13).

This mathematical derivation shows that five moments of the ODF can be obtained from the measurement of five reduced fluorescence intensities. Experimental measurements of fluorescence intensities do not lead directly to reduced values. In fact, more than five intensities must be measured so that ratios of intensities can be calculated and the instrumental constant K can be eliminated. In the next section, we present an experimental method to obtain the 3×3 matrix of fluorescence intensities I_{ij} characterizing biaxial media.

EXPERIMENTAL MEASUREMENTS OF FLUORESCENCE INTENSITIES

Principle

In order to measure an intensity I_{ij} (where $i, j \in (1, 2, 3)$), the directions of the polarizer P and the analyser A must have a non-zero projection on the i and j axis respectively. This basic principle led us to adopt the following experimental design and method.

Experimental set-up

A schematic representation of the apparatus is given in *Figure 2*. The laboratory frame $0xyz$ is indicated in *Figure 2*. The plane of incidence is the $z0y$ plane, and it is identical for both excitation and emission. The sample is placed on a horizontal holder which rotates around the z axis so that the X_3 direction of the sample lies along the z axis. The X_1 or X_2 directions can be set parallel to the x or y axis. The direction of the monochromatic excitation light makes an angle α with the z axis and the fluorescence emission is analysed at an angle β with the same axis. As is conventionally done, we define the s polarization as the polarization perpendicular to the plane of incidence (i.e. in the x direction) and the p polarization as the polarization parallel to the plane of incidence. A polarized fluorescence intensity is obtained by setting the polarizer and the analyser parallel to either p or s. Therefore, for a given pair α and β, four intensities (I_{pp}, I_{ps}, I_{sp}, I_{ss}) can be measured.

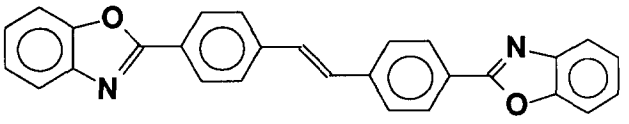

Figure 3 4,4'-(Dibenzoxazolyl)stilbene (VPBO)

In order to eliminate unknown parameters in the experimental constant K (like excitation intensity), ratios of polarized fluorescence intensities corresponding to the same excitation polarization, rather than absolute values of intensities, must be considered. Moreover, experimental artifacts such as short- and long-term fluctuations of the excitation intensity can be eliminated by using a Wollaston prism. It is adjusted so that one of its principal directions lies parallel to the x axis, affording a simultaneous measurement of the p and s polarizations of the fluorescence emission. Such a use of a Wollaston prism in polarized fluorescence intensity measurements has already been described[31]. Two sets of conveniently chosen α and β values are sufficient to measure the required number of intensities.

Using $\beta=0$ and $\alpha=45°$, four ratios are obtained. The choice of the s polarization in excitation directly leads to I_{11}/I_{12} and I_{22}/I_{12} by setting the sample with axis X_1 parallel to x and y respectively. If now the p polarization is considered, I_{13}/I_{12} and I_{23}/I_{12} can be deduced from the measured intensities using the values of the first two ratios determined previously. A detailed demonstration of this methodology is given in the Appendix.

In order to measure I_{33} accurately, the sample must be positioned symmetrically with regard to the excitation and analysis directions. In addition, the component of the directions of the polarizer and analyser along the X_3 axis must be maximized. A grazing incidence is unfavourable due to high Fresnel reflection coefficients, which depend strongly upon the angle of incidence and the refractive index. We therefore choose $\alpha=\beta=67.5°$. As explained in the Appendix, the intensity measurements allow I_{33}/I_{12} to be calculated using the values of the previous ratios.

Birefringence and crystallinity effects

Birefringence corrections are often required in FP measurements[14]. The differences of the refractive indices along the three principal axes of the sample induce, *a priori*, three corrections.

The most obvious one is related to the incidence angle inside the material, governed by Descartes law. This correction is completely negligible under our conditions of birefringence.

The second one is related to the change in the reflection and transmission coefficients at the air–sample interface. The coefficients can vary with the direction of polarization with respect to the principal axes. Here, the highest birefringence is of the order of 2×10^{-1} for an average index of 1.574. The maximum deviation of the ratio $\tau_p(67.5°)/\tau_s(67.5°)$ is therefore approximately 5% (τ_p and τ_s are the Fresnel intensity transmission coefficients involved in the calculation of I_{33}/I_{12} (see the Appendix)). We decided not to take this correction into account since it will always be less than 5%. For the configuration $\alpha=45°$ and $\beta=0°$, the correction is even smaller (less than 0.5%).

The third effect of birefringence is to introduce a phase difference between two polarizations of a light propagating in the same direction along two different principal axes. Although this effect can be evaluated[14], this situation is not encountered with our experimental method. Indeed, all the directions of polarization coincide with a principal axis of the refractive index ellipsoid for the direction of propagation considered.

Crystallinity causes depolarization of both the excitation light and emitted fluorescence. This effect appears when light scattering phenomena occur, which can be easily checked using a small-angle light scattering device. The samples investigated in this study show little or no scattering. This phenomenon has been confirmed by X-ray diffraction measurements which indicate a relatively small crystal size (less than (5 nm)[3]), although the crystallinity can reach a value of 20%. We therefore believe that our intensity measurements are not significantly affected by the depolarization due to the crystallites.

TEST OF THE METHOD

In the final part, we present experimental results obtained on isotropic, uniaxially and biaxially oriented PET films.

Experimental

Amorphous, isotropic PET films (thickness 160 μm), obtained by quenching an extruded film on a cold roll, were supplied by Rhône-Poulenc Recherches. The weight-average molecular weight was 39 000 as determined by viscosimetry in *o*-chlorophenol at 25°C. T_g was 80°C as measured by d.s.c. at 20°C min^{-1}.

The uniaxially oriented samples were obtained by stretching the isotropic ones at 0.028 s^{-1} and 90°C on a hydraulic stretching machine developed in our laboratory[32].

Biaxially oriented samples have been provided by Rhône-Poulenc Films. Although these films possess an orthorhombic symmetry, the term 'biaxial' does not properly qualify these samples since only longitudinal stretching (MD) at constant width has been applied. The films with different draw ratios were stretched under the same temperature conditions.

In order to allow fluorescence measurements, care was taken during the polymerization to minimize intrinsic fluorescence, and a photostable compound, 4,4'-(dibenzoxazolyl)stilbene (VPBO) (Eastobrite OB1, Eastman Kodak) (see *Figure 3*), was added during the polycondensation at a concentration of 100 ppm (by weight).

The fluorescence intensities were measured on an apparatus developed in our laboratory[33]. The general design of the equipment is shown in *Figure 2*.

Principal refractive indices of the sample were measured using an Abbe refractometer, and the degree of crystallinity was determined from density measurements by the relation:

$$\chi=\frac{d-d_a}{d_c-d_a}$$

with $d_c=1.455$ and $d_a=1.335$. The physical characterization of the samples is summed up in *Table 1*.

As determined above, fluorescence intensity measurements lead to the determination of the 3×3 I_{ij} matrix. As an example, we have listed below the matrices obtained for the isotropic, uniaxial and biaxial 3.0

Table 1 Physical characterization of the investigated PET samples

Type of orientation		Draw ratio, X_1-X_2-X_3	Crystallinity (%)	Refractive indices		
				n_1	n_2	n_3
Isotropic		1-1-1	0	1.5758	1.5752	1.5735
Uniaxial		3-0.58-0.58	7	1.6108	1.5621	1.5618
Biaxial	3.0	3-1-0.33	0	1.6210	1.5635	1.5506
	3.2	3.2-1-0.31	3	1.6320	1.5652	1.5468
	3.4	3.4-1-0.29	10	1.6360	1.5688	1.5393
	3.6	3.6-1-0.28	16	1.6656	1.5712	1.5258

samples (the I_{12} intensity has been set to 1):

(i) Isotropic sample

$$\begin{pmatrix} 2.24 & 1 & 0.88 \\ 1 & 2.21 & 0.84 \\ 0.88 & 0.84 & 2.12 \end{pmatrix}$$

(ii) Uniaxial sample

$$\begin{pmatrix} 4.66 & 1 & 0.71 \\ 1 & 1.17 & 0.33 \\ 0.71 & 0.33 & 1.14 \end{pmatrix}$$

(iii) Biaxial 3.0 sample

$$\begin{pmatrix} 5.51 & 1 & 0.46 \\ 1 & 0.86 & 0.18 \\ 0.46 & 0.18 & 0.66 \end{pmatrix}$$

The uncertainty in the measurements is ± 0.02 for I_{11} and I_{22}, ± 0.03 for I_{13} and I_{23} and ± 0.1 for I_{33}.

These matrices deserve several comments. First, the existence of a molecular orientation appears directly in the fluorescence intensities. I_{11} increases significantly in the uniaxially and biaxially oriented samples, reflecting a higher orientation of the probes along the X_1 axis. Consequently, I_{22} and I_{33} decrease.

A careful examination of the matrix for the isotropic sample shows that this film is not strictly isotropic. Indeed, the theoretical matrix for an isotropic film would be:

$$\begin{pmatrix} 2.22 & 1 & 1 \\ 1 & 2.22 & 1 \\ 1 & 1 & 2.22 \end{pmatrix}$$

(The value 2.2 (rather than 3) for the diagonal terms is obtained due to the delocalization of the absorption and emission transition moments.) The 1,2 submatrix, which characterizes the plane of the film, is very close to the theoretical one. This point shows that the film is effectively isotropic with respect to the directions 1 and 2. This point is further confirmed by the refractive index measurements. On the other hand, by looking at the values of the I_{13} intensities, one can see that this film is not isotropic in direction 3. Such a feature can be ascribed to the processing history of the sample, since the extrusion process may induce the orientation in the film.

The uniaxial sample is obtained by stretching the isotropic one. The corresponding matrix shows that the dissymmetry between directions 2 and 3 already present in the parent sample remains even after stretching ($I_{13} \neq I_{23}$). Although I_{22} is close to I_{33}, the 2,3 submatrix is not strictly isotropic either. This observation is confirmed by the refractive indices.

In the case of the biaxially oriented sample, a noticeable difference exists between I_{22} and I_{33}, indicating that the fluorescent probe tends to align preferentially in the plane of the film. This is corroborated by the strong decrease of the intensity I_{13} with respect to I_{12}.

From these matrices, the P_{lm0} values can be easily calculated using equation (14). They are tabulated for the various samples in *Table 2*. Before discussing these results, a brief comment about the validity of the assumption concerning an axial symmetry of M_a and M_e around M_0 is of value.

This assumption fails if there is a preferential orientation of a normal to the long axis of the VPBO molecule with respect to the plane of the film, i.e. the probe behaves like a 'blade' rather than a rod. This may happen in our case, if there is a marked orientation of the phenyl rings with respect to the plane of the sheet, or if the probes, instead of being located randomly in the amorphous phase, tend to stick to the external faces of the crystallites. Recent studies in our laboratory, combining X-ray diffraction, trirefringence and fluorescence polarization measurements, indicate that a strong orientation of the phenyl rings is present in the crystalline phase, but that it remains quite weak in the amorphous phase. Moreover, the behaviour of the amorphous phase, seen through the orientation of the VPBO molecules, appears completely different from that of the crystalline phase. So, our assumption concerning the transition moments seems at least a good approximation.

Table 2 confirms that the 'isotropic' sample is not strictly isotropic. A small orientation in the extrusion direction can be noted ($P_{200}=0.015$) together with a planar symmetry as indicated by the P_{220} value. This quantity is very sensitive to any preferential ordering in the 2,3 plane. In the uniaxial sample, a high level of orientation along the X_1 axis can be seen ($P_{200}=0.42$). The orientation in the 2,3 plane is slightly more marked than in the isotropic state ($P_{220}=0.008$). The most interesting feature appears in the biaxially oriented films with different extension ratios. *Table 2* indicates that a very high orientation along the MD gradually develops as the draw ratio increases together with a higher orientation along the 2 direction in the 2,3 plane. It should be noted that the P_{420} and P_{440} values are constant in this range of draw ratios.

Our P_{lm0} values can be compared with other published data[4]. P_{200} and P_{400} obtained from fluorescence intensity measurements are higher than that found by Raman spectroscopy. This can be explained by the fact that our fluorescence measurements are related to an extrinsic

Table 2 Values of the different orientation averages

Type of orientation		P_{200}	P_{220}	P_{400}	P_{420}	P_{440}
Isotropic		0.015	0.004	0.006	0.003	0.006
Uniaxial		0.42	0.008	0.24	0.008	0.013
Biaxial	3.0	0.58	0.017	0.42	0.016	0.015
	3.2	0.62	0.020	0.44	0.017	0.016
	3.4	0.72	0.027	0.56	0.018	0.016
	3.6	0.89	0.033	0.65	0.018	0.015

probe. Indeed, it has been shown for uniaxial extension that the VPBO molecule reflects the orientation of amorphous chains in the *trans* conformation[19] and not the average amorphous orientation. A higher value can thus be expected. As far as the P_{220} value is concerned, it can be noted that our FP values are also slightly higher than those obtained by Raman spectroscopy. However, they are close to that predicted by a pseudo-affine deformation model for similar draw ratios. This deformation scheme seems very conceivable for rod-like molecules.

CONCLUSIONS

In this paper, we have presented a reliable experimental method to measure six fluorescence intensities required to characterize fully the orientation in a biaxially oriented sample. A mathematical treatment has been developed to allow calculation of five moments of the orientation distribution function from these intensity measurements.

ACKNOWLEDGEMENTS

We gratefully acknowledge Professor I. M. Ward for kindly providing us with VPBO and Rhône-Poulenc Films for supplying biaxially oriented samples and for providing a Ph.D. fellowship to one of us (Ph.L.).

REFERENCES

1 De Vries, A. J., Bonnebat, C. and Beautemps. J. *J. Polym. Sci., Polym. Symp.* 1977, **58**, 109
2 Jarvis, D. A., Hutchinson, I. J., Bower, D. I. and Ward, I. M. *Polymer* 1980, **21**, 41
3 Jabarin, S. A. *Polym. Eng. Sci.* 1984, **24**, 376
4 Bower, D. I., Jarvis, D. A. and Ward, I. M. *J. Polym. Sci., Polym. Phys. Edn.* 1986, **24**, 1459
5 Ward, I. M. *Adv. Polym. Sci.* 1985, **66**, 81
6 Harbison, G. S., Vogt, V. D. and Spiess, H. W. *J. Chem. Phys.* 1987, **86**, 1206
7 Henrichs, P. M. *Macromolecules* 1987, **20**, 2099
8 Koenig, J. L. and Cornell, S. W. *J. Macromol. Sci.–Phys. (B)* 1967, **1**, 279
9 Fina, L. J. and Koenig, J. L. *J. Polym. Sci., Polym. Phys. Edn.* 1986, **24**, 2509
10 Jungnickel, B. J., Teichgräber, M. and Rucher, C. *Faserforsch. Textiltech.* 1973, **24**, 423
11 Huisman, R. and Henvel, H. M. *J. Appl. Polym. Sci.* 1978, **22**, 943
12 Jungnickel, B. *J. Angew. Makromol. Chem.* 1980, **91**, 203
13 Cakmak, M., White, J. L. and Spruiell, J. E. *J. Polym. Eng.* 1986, **6**, 291
14 Jarry, J. P. and Monnerie, L. *J. Polym. Sci., Polym. Phys. Edn.* 1978, **16**, 443
15 Le Bourvellec, G., Monnerie, L. and Jarry, J. P. *Polymer* 1986, **27**, 855
16 Bower, D. I. *J. Polym. Sci., Polym. Phys. Edn.* 1972, **10**, 2135
17 Nobbs, J. H., Bower, D. I., Ward, I. M. and Patterson, D. *Polymer* 1974, **15**, 287
18 Nobbs, J. H., Bower, D. I. and Ward, I. M. *Polymer* 1976, **17**, 25
19 Nobbs, J. H., Bower, D. I. and Ward, I. M. *J. Polym. Sci., Polym. Phys. Edn.* 1979, **17**, 259
20 Bower, D. I., Korybut-Daskiewicz, K. K. P. and Ward, I. M. *J. Appl. Polym. Sci.* 1983, **28**, 1195
21 McGraw, G. E. *J. Polym. Sci. (A2)* 1970, **8**, 1323
22 Nishijima, Y., Onogi, Y. and Asai, T. *J. Polym. Sci. (C)* 1966, **15**, 237
23 Nishijima, Y. *J. Polym. Sci. (C)* 1970, **31**, 353
24 Hennecke, M., Kud, A., Kurz, K. and Furhmann, J. *Colloid Polym. Sci.* 1987, **265**, 674
25 Hemker, D. J., Frank, C. W. and Thomas, J. W. *Polymer* 1988, **29**, 437
26 Ward, I. M. 'Structure and Properties of Oriented Polymers', Applied Science, London, 1975
27 Bower, D. I. *J. Polym. Sci., Polym. Phys. Edn.* 1981, **19**, 93
28 Bower, D. I. *Polymer* 1982, **23**, 1251
29 Monnerie, L. in 'Static and Dynamic Properties of the Polymeric Solid State' (Eds. R. A. Pethrick and R. W. Richards), Reidel, London, 1981
30 Desper, C. R. and Kimura, I. *J. Appl. Phys.* 1967, **38**, 4225
31 Teissié, J., Valeur, B. and Monnerie, L. *J. Phys. (E), Sci. Instrum.* 1975, **8**, 700
32 Fajolle, R., Tassin, J. F., Sergot, Ph., Pambrun, C. and Monnerie, L. *Polymer* 1983, **24**, 379
33 Sergot, Ph., Doctoral Thesis, Université Paris VI, 1976

APPENDIX

We have used the tensorial formalism of Desper and Kimura[30] to calculate the expression of any fluorescence intensity as a function of the components of the 3×3 matrix. Although this formalism is based on the assumption $\boldsymbol{M}_a = \boldsymbol{M}_e = \boldsymbol{M}_0$, it can be extended to the more general case. Indeed, any fluorescence intensity can be written:

$$I(\boldsymbol{P}, \boldsymbol{A}) = K \langle (\boldsymbol{P}.\boldsymbol{M}_a)^2 (\boldsymbol{M}_e.\boldsymbol{A})^2 \rangle$$

$\boldsymbol{P}$ and $\boldsymbol{A}$ can be decomposed as:

$$\boldsymbol{P} = \sum_{i=1}^{3} P_i \boldsymbol{X}_i \qquad \text{and} \qquad \boldsymbol{A} = \sum_{j=1}^{3} A_j \boldsymbol{X}_j$$

so that:

$$I_{PA} = \frac{I(\boldsymbol{P}, \boldsymbol{A})}{K} = \sum_{i=1}^{3} \sum_{j=1}^{3} P_i^2 A_j^2 \langle (\boldsymbol{X}_i.\boldsymbol{M}_a)^2 (\boldsymbol{X}_j.\boldsymbol{M}_e)^2 \rangle$$

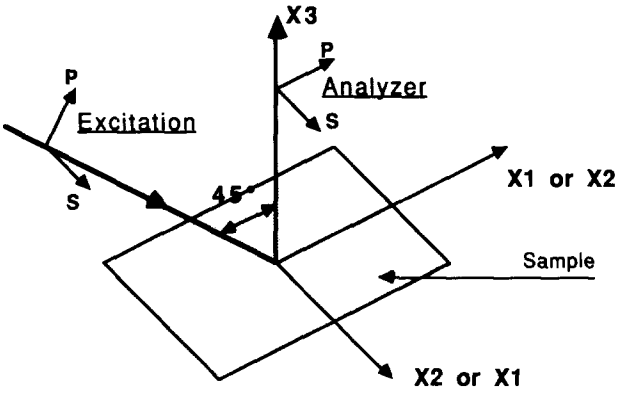

Figure 4 Experimental arrangement to determine the ratios I_{13}/I_{12} and I_{23}/I_{12}

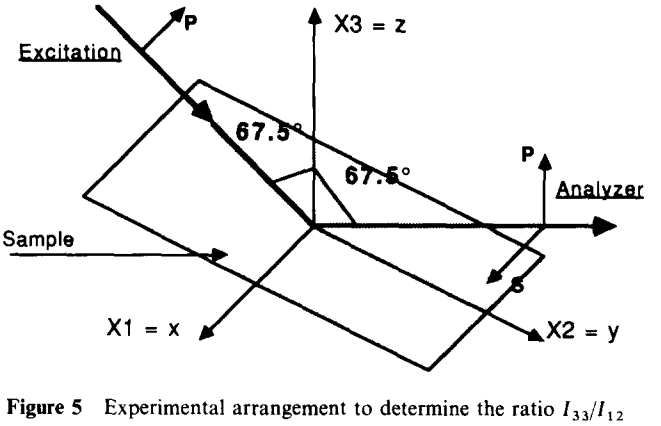

Figure 5 Experimental arrangement to determine the ratio I_{33}/I_{12}

The term $\langle (X_i.M_a)^2 (X_j.M_e)^2 \rangle$ is in fact the reduced intensity I_{ij} when M_a and M_e do not coincide.

As an example, we give the expression of the measured intensities as a function of the terms of the I_{ij} matrix for the experimental arrangement shown in *Figure 4*. It can easily be shown that:

$$I_{pp} = K[(\cos^2\theta')I_{11} + (\sin^2\theta')I_{13}]$$

$$I_{ps} = K[(\cos^2\theta')I_{12} + (\sin^2\theta')I_{23}]$$

where $\theta' = \sin^{-1}[(\sin 45°)/n]$ is the incidence angle inside the material, and n is the average refractive index of the sample. If the sample is rotated 90° around the X_3 axis, the measurement of I_{pp} and I_{ps} combined with the previous one allows calculation of I_{13}/I_{12} and I_{23}/I_{12}.

The experimental arrangement for measuring I_{33} is presented in *Figure 5*. It can be shown that:

$$\frac{I_{pp}}{I_{ps}} = \frac{\tau_p(67.5)}{\tau_s(67.5)} \times \frac{[(\sin^4\theta')I_{33} + (\cos^4\theta')I_{22} - 2(\sin^2\theta'\cos^2\theta')I_{23}]}{[(\sin^2\theta')I_{13} + (\cos^2\theta')I_{12}]}$$

where $\theta' = \sin^{-1}[(\sin 67.5°)/n]$. τ_p and τ_s are the intensity transmission coefficients for p and s polarized waves at an angle of incidence of 67.5°. From the above expression, one can determine the ratio I_{33}/I_{12}.